



Synthesis, structure, photochromism and DFT calculations of copper(I)-triphenylphosphine halide complexes of thioalkylazoimidazoles

Gunomoni Saha^{a,1}, Papia Datta^a, Kamal Krishna Sarkar^b, Rajat Saha^c, Golam Mostafa^c, Chittaranjan Sinha^{a,*}

^a Department of Chemistry, Inorganic Chemistry Section, Jadavpur University, Kolkata 700 032, India

^b Department of Chemistry, Mahadevananda Mahavidyalaya, Barrackpore, Monirampore, Kolkata 700 120, India

^c Department of Physics, Jadavpur University, Kolkata 700 032, India

ARTICLE INFO

Article history:

Received 30 September 2010

Accepted 25 November 2010

Available online 7 December 2010

Keywords:

Copper(I)-thioalkylazoimidazole-halide

X-ray structure

Photochromism

Electrochemistry

DFT computation

ABSTRACT

[Cu(SRaaNR')(PPh₃)X] complexes are synthesized by the reaction of CuX (X = Cl, Br, I), triphenylphosphine and 1-alkyl-2-[(*o*-thioalkyl)phenylazo]imidazole (SRaaNR'). The single crystal X-ray structure of [Cu(SEtaaNH)(PPh₃)I] (SEtaaNH = 2-[(*o*-thioethyl)phenylazo]imidazole) shows a distorted tetrahedral geometry of the copper center with bidentate, N(azo), N(imidazole) chelation of SEtaaNH and coordination from PPh₃ and iodine. These complexes show a *trans*-to-*cis* isomerization upon irradiation with UV light. The reverse transformation, *cis*-to-*trans* isomerization, is very slow with visible light irradiation and is thermally accessible. The quantum yields ($\phi_{t \rightarrow c}$) of the *trans*-to-*cis* isomerization of [Cu(SRaaNR')(PPh₃)X] are lower than the free ligand values. This is due to the increased mass and rotor volume of the complexes compared to the free ligand data. The rate of isomerization follows the order: [Cu(SRaaNR')(PPh₃)Cl] < [Cu(SRaaNR')(PPh₃)Br] < [Cu(SRaaNR')(PPh₃)I]. The activation energy (E_a) of the *cis*-to-*trans* isomerization is calculated by a controlled temperature reaction. DFT computation of representative complexes has been used to determine the composition and energy of the molecular levels.

© 2010 Elsevier Ltd. All rights reserved.

1. Introduction

Azobenzene displays reversible photoisomerization and the derivatives are very useful as an optical response function (trigger and switching) molecule, because the molecular shape and polarity greatly change on optical illumination [1–7]. This has inspired changing either or both aryl rings of azobenzene with heterocycles and to explore their photophysical properties as well as the influence of metal coordination or protonation. (Arylazo)heterocycles which bear pyridine, pyrimidine, imidazole or pyrazole rings have been extensively utilized in the field of coordination chemistry owing to their chelation by N(heterocycle) and N(azo) to a metal ion [8–12]. Many of them also exhibit *trans*-to-*cis* (Z–E) photoisomerization, and the coordination ability of the heterocyclic moiety can be changed by the photoisomerization. This activity has immense application in the design of light driven on-off switching [13,14]. Arylazoimidazoles constitute an interesting class of heterocyclic azo compounds as a potential switching group in biological applications and in coordination chemistry, since imidazole is a ubiquitous and essential group in biology, especially as a metal

coordination site. This family of compounds has been extensively used as ligands to synthesize transition and non-transition metal complexes [15–22]. The photochromism of 1-alkyl-2-(ary-lazo)imidazole (RaaNR') [10,11] and some complexes like Hg(II)-[23] Cd(II)- [24] and Pd(II)-azoimidazoles [25] have been reported by our group. To extend the chemistry of azoimidazoles we have synthesized 1-alkyl-2-[(*o*-thioalkyl)phenylazo]imidazoles (SRaaNR') (2 and 3) [26]. The reaction of CuX with SRaaNR' in the presence of PPh₃ has isolated [Cu(SRaaNR')(PPh₃)X] (4–9). The structure is confirmed by a single crystal X-ray diffraction study in one case and also by other spectroscopic studies. The photochromic property of the complexes is also examined. Quantum chemical calculations using density functional theory (DFT) have been carried out to explain the structural, electronic, spectroscopic and thermodynamic properties of the different compounds. Time-dependent density functional theory (TD-DFT) is opening new perspectives in this field [27,28], so DFT computations have been used to correlate the UV–Vis spectral and redox properties of the complexes.

2. Results and discussion

2.1. Synthesis and formulation

The 1-alkyl-2-[(*o*-thioalkyl)phenylazo]imidazoles (SRaaNR') (2 and 3) are synthesized by the reported procedure [26] (Scheme

* Corresponding author.

E-mail address: c_r_sinha@yahoo.com (C. Sinha).

¹ Present address: Department of Chemistry, Barrackpore Rastraguru Surendranath College, Barrackpore, Kolkata 700 120, India.

1). The reaction of CuX and the appropriate ligand, SRaaiNR' in a 1:1 mole ratio in methanol, followed by the addition of one equivalent of PPh₃ has isolated [Cu(SRaaiNR')(PPh₃)X] (**4–9**). The reaction was also carried out with [Cu(PPh₃)X]₄ and SRaaiNR', and the same complex was isolated. However, the process is not fast and we followed the reaction *in situ*. The complexes are purified by crystallization, on slow evaporation of a solution in acetonitrile–methanol (1:1, v/v). Microanalytical data have confirmed the composition of the complexes. The complexes are sufficiently soluble in common organic solvents, viz. methanol, ethanol, chloroform, dichloromethane and acetonitrile, but are insoluble in hydrocarbons (hexane, benzene, and toluene). They are non-conducting in methanol/acetonitrile solution.

2.2. Spectral studies

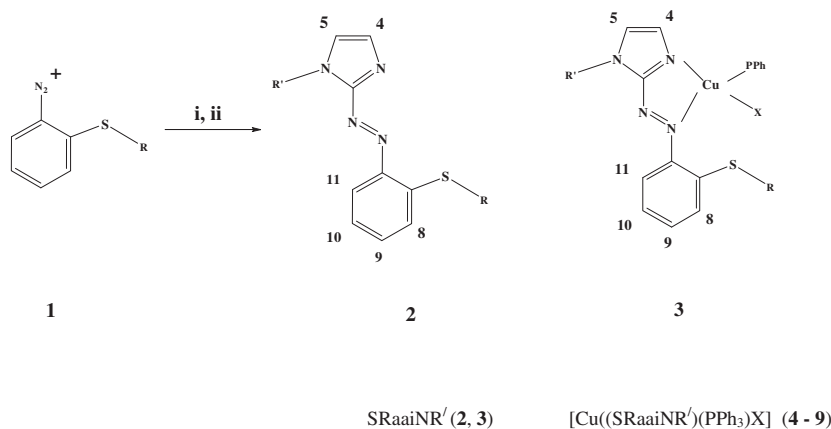
Infrared spectra of the complexes exhibit $\nu(\text{N}=\text{N})$ and $\nu(\text{C}=\text{N})$ at 1412–1431 and 1580–1597 cm⁻¹, respectively. These two specific frequencies, $\nu(\text{N}=\text{N})$ and $\nu(\text{C}=\text{N})$, are red shifted by 10–12 cm⁻¹ in the complexes compared to the free ligand values. This supports coordination of azo-N and imine-N to Cu(I).

The UV–Vis spectra of the complexes exhibit three or four high intense transitions ($\epsilon \sim 10^4 \text{ M}^{-1} \text{ cm}^{-1}$) at 450–465, 400–420, 355–365 and 245–260 nm, along with a weak transition at 600–620 nm ($\epsilon \sim 10^3 \text{ M}^{-1} \text{ cm}^{-1}$) (Fig. 1). The free ligand SRaaiNR' shows intraligand charge transferances, $n-\pi^*$ and $\pi-\pi^*$, at 370–380 and 250–260 nm respectively [26]. Thus the transitions > 400 nm are assigned to Cu(I) $\rightarrow \pi^*(\text{azo})$. The transitions are characterized based on an electronic structure calculation using an optimized geometry by the DFT computation technique (*vide infra*).

The ¹H NMR spectral data (Supplementary Material, Table S1) have been used to determine the stereochemistry of the complexes. The aryl and imidazole protons are downfield shifted on coordination of the ligand to the Cu(I) center compared to the free ligand data [26]. This implies a significant bonding interaction of the metal ion with the ligand, which effectively influences the ligand's electron density. The S–R and N(1)–R' groups show the usual spin–spin interaction pattern in the upper field portion of the aliphatic region in the NMR spectra.

2.3. Crystal structure of [Cu(SEtaaiNH)(PPh₃)I] (**9a**)

The molecular structure of [Cu(SEtaaiNH)(PPh₃)I] (**9a**) is shown in Fig. 2. The bond parameters are listed in Table 1. The chelating ligand, SEtaaiNH, acts as a N,N'-donor (N refers to N(imidazole) and N' refers to N(azo)), and the two other donor centers are PPh₃ and I. The –S–Et group remains uncoordinated and away from the metal center. The atomic arrangements Cu, N(4), N(3), C(3), N(1), constitute a chelate plane with a deviation < 0.02 Å. Cu(I) is at the center of a distorted tetrahedron. The pendant aryl ring makes a dihedral angle of 2.3(5)° with the chelated azoimidazole ring. The acute bite angle, Cu(N, N'), of 77.42(18)° is extended by SEtaaiNH on coordination to Cu(I) and is comparable with reported results in the series of chelated arylazoimidazole complexes of d¹⁰ metal complexes [29,9,30]. The small chelate angle may be one of the reasons for geometrical distortion. The Cu–N(azo) bond length (2.163(5) Å), is longer than the Cu(I)–N(imidazole) bond length (2.088(5) Å), which reflects the stronger interaction of Cu(I) with N(imidazole) compared to N(azo). The N=N distance is



i) imidazole in pH, 7; ii) NaH in THF and R'I

R = Me, R' = H (**2a**), R = Me, R' = Me (**2b**);

R = Me, R' = Et (**2c**), R = Et, R' = H (**3a**);

R = Et, R' = Me (**3b**), R = Et, R' = Et (**3c**)

Abbreviations of **a, b, c** remain the same.

X = Cl (**4, 5**); Br (**6, 7**); I (**8, 9**)

[Cu(SMeaaiNH)(PPh₃)Cl] (**4a**), [Cu(SMeaaiNMe)(PPh₃)Cl] (**4b**), [Cu(SMeaaiNEt)(PPh₃)Cl] (**4c**),

[Cu(SEtaaiNH)(PPh₃)Cl] (**5a**), [Cu(SEtaaiNMe)(PPh₃)Cl] (**5b**), [Cu(SEtaaiNEt)(PPh₃)Cl] (**5c**)

[Cu(SMeaaiNH)(PPh₃)Br] (**6a**), [Cu(SMeaaiNMe)(PPh₃)Br] (**6b**), [Cu(SMeaaiNEt)(PPh₃)Br] (**6c**),

[Cu(SEtaaiNH)(PPh₃)Br] (**7a**), [Cu(SEtaaiNMe)(PPh₃)Br] (**7b**), [Cu(SEtaaiNEt)(PPh₃)Br] (**7c**)

[Cu(SMeaaiNH)(PPh₃)I] (**8a**), [Cu(SMeaaiNMe)(PPh₃)I] (**8b**), [Cu(SMeaaiNEt)(PPh₃)I] (**8c**),

[Cu(SEtaaiNH)(PPh₃)I] (**9a**), [Cu(SEtaaiNMe)(PPh₃)I] (**9b**), [Cu(SEtaaiNEt)(PPh₃)I] (**9c**)

Scheme 1.

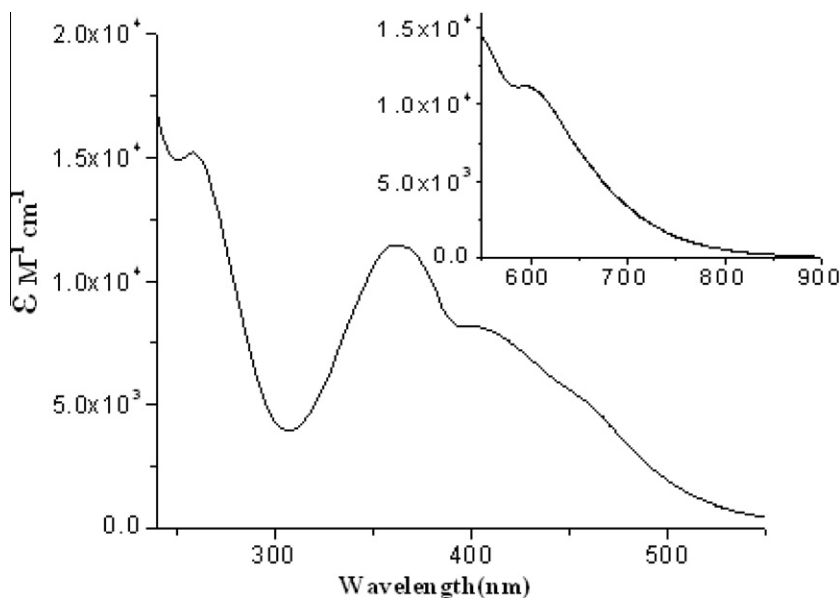


Fig. 1. UV-Vis spectrum of $[\text{Cu}(\text{SMeaaiNEt})(\text{PPh}_3)\text{Cl}]$ (**4c**) in acetonitrile.

1.286(6) Å. This is elongated by a small amount compared to that of the free ligand value (1.252(1) Å) [10].

C–H $\cdots\pi$ and $\pi\cdots\pi$ interactions are observed in the packing of the crystal to generate 1D (Fig. 3) and 2D (Fig. 4) supramolecular structures. The interactions are observed between the Cu(N, N') plane and the imidazole ring (Cg(2)) of two adjacent molecules (Cu(N, N') \cdots Cg(2)(imidazole), 3.721 Å; symmetry, $-x, -y, -z$ and x, y, z respectively). The $\pi\cdots\pi$ interactions are observed in Cg(2)–Cg(3) at 3.562(6) Å (Cg(3): C(4)–C(5)–C(6)–C(7)–C(8)–C(9); symmetry, $1+x, y, z$). The phenyl rings of PPh₃ interact with the partners of a neighboring molecule and the C–H $\cdots\pi$ distance is 2.93 Å; angle 159°, symmetry, $x, -1+y, z$ and 2.99 Å; angle 154°, symmetry, $1+x, y, z$. The pendant aryl-SR group also interacts with C(11)–H(9), at a distance of 2.96 Å, angle 140°, symmetry, $2-x, -y, 1-z$ (Supplementary Material, Table S2). These interactions increase the intermolecular attraction to generate a π -network (Fig. 4).

2.4. Electrochemistry

The redox activity of the compounds is examined by the cyclic voltammogram technique. Fig. 5 shows the cyclic voltammograms of the copper(I) complexes in MeCN at a Pt-disk milli electrode in the potential range +1.5 to –1.8 V versus a SCE reference electrode (Supplementary material, Table S3). An oxidative response is observed at 0.4 V. The quasireversibility is proved by the peak-to-peak separation ($\Delta E_p > 100$ mV) and the response is assigned to Cu(II)/Cu(I). On scanning to the –ve direction up to –1.8 V, we observe an irreversible response E_{pc} at –0.4 V and a quasireversible response at –1.1 to –1.3 V ($\Delta E_p > 140$ mV). These may be assigned to the reduction of the azo group $[(-\text{N}=\text{N})/(-\text{N}=\text{N}^-)]$ of the chelated ligands. The voltammograms also show a sharp anodic part at ~ -0.2 V, possibly due to the Cu(I)/Cu(0) couple [26,30]. Reduced Cu(0) is absorbed on the electrode surface, as evidenced from the

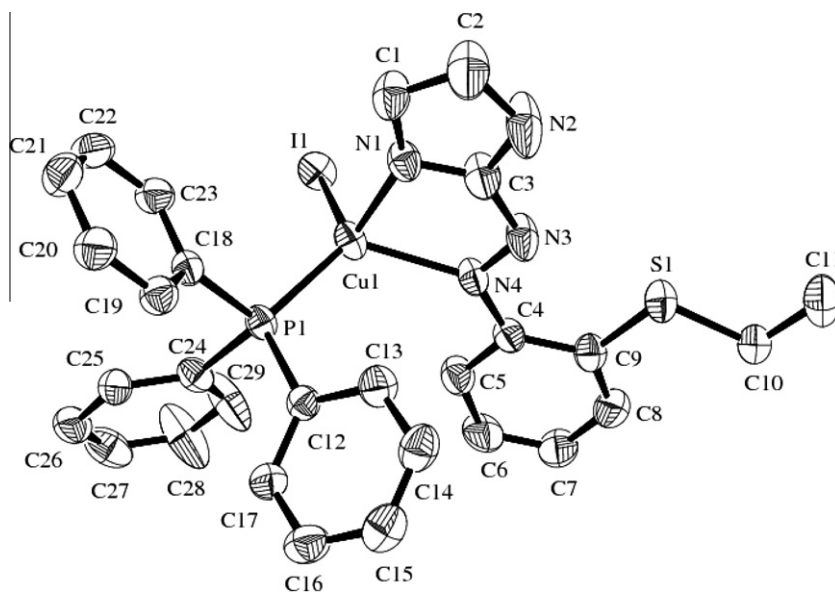
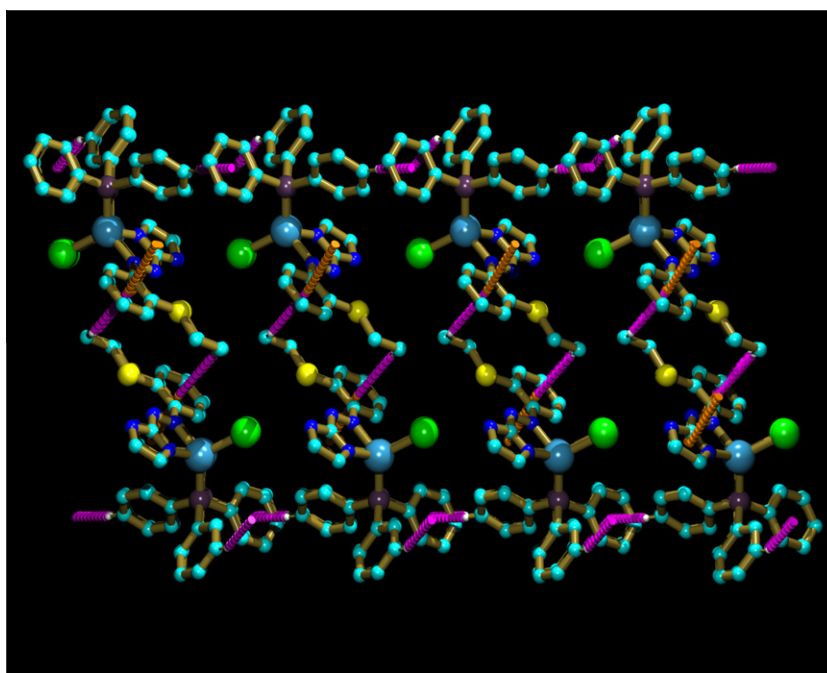


Fig. 2. The ORTEP diagram of $[\text{Cu}(\text{SEtaaiNH})(\text{PPh}_3)\text{I}]$ (**9a**) with 30% probability.

Table 1
Bond distances and bond angles of [Cu(SEtaaiNH)(PPh₃)] (**9a**).

	X-ray	Theo ^a		X-ray	Theo ^a
<i>Bond distance (Å)</i>					
Cu(1)–N(1)	2.088(5)	2.12168	N(1)–C(3)	1.292(12)	1.403
Cu(1)–N(4)	2.163(5)	2.14459	P(1)–C(12)	1.814(8)	1.88766
Cu(1)–I(1)	2.5596(9)	2.63375	P(1)–C(18)	1.778(4)	1.88766
Cu(1)–P(1)	2.2108(15)	2.40883	P(1)–C(24)	1.831(8)	1.888
N(3)–N(4)	1.286(6)	1.31151	C(4)–N(4)	1.401(7)	1.41544
<i>Angles (°)</i>					
I(1)–Cu(1)–P(1)	119.65(5)	110.9872	N(1)–Cu–N(4)	77.42(18)	78.13
I(1)–Cu(1)–N(1)	111.02(15)	117.5242	C(12)–P(1)–Cu(1)	114.40(17)	108.5
I(1)–Cu(1)–N(4)	110.48(13)	114.9913	Cu(1)–P(1)–C(18)	111.10(18)	103.4
P(1)–Cu(1)–I(1)	112.66(14)	108.7570	Cu(1)–P(1)–C(24)	119.02(18)	112.7
P(1)–Cu(1)–N(4)	118.01(14)	122.6451			

^a Theoretically calculated data are obtained from the optimized geometry of the complex using the DFT computation technique.

**Fig. 3.** 1D pattern due to C–H··· π interactions of [Cu(SEtaaiNH)(PPh₃)] (**9a**).

narrow width of the anodic response with a large peak current. Carrying out the experiment with a back scan going to a negative potential of -0.6 V does not produce such a large anodic current at -0.2 V.

2.5. Photo response of [Cu((S)RaaiNR')(PPh₃)X]

The effect of UV-light irradiation to an acetonitrile solution of [Cu((S)RaaiNR')(PPh₃)X] is shown in Fig. 6 (Scheme 2). The irradiation wavelength and its quantitative effect are given as Supplementary material, Table S4. The irradiation wavelength is ascribed to the π – π^* transition of the azo moiety in the *trans* form, at 364 nm ($14\,530\text{ M}^{-1}\text{ cm}^{-1}$) (**4b**), 361 nm ($11\,421\text{ M}^{-1}\text{ cm}^{-1}$) (**4c**), 357 nm ($8842\text{ M}^{-1}\text{ cm}^{-1}$) (**5b**), 365 nm ($18\,950\text{ M}^{-1}\text{ cm}^{-1}$) (**5c**), 358 nm ($12\,220\text{ M}^{-1}\text{ cm}^{-1}$) (**6b**), 359 nm ($14\,561\text{ M}^{-1}\text{ cm}^{-1}$) (**6c**), 361 nm ($11\,930\text{ M}^{-1}\text{ cm}^{-1}$) (**7b**), 363 nm ($13\,479\text{ M}^{-1}\text{ cm}^{-1}$) (**7c**), 363 nm ($13\,340\text{ M}^{-1}\text{ cm}^{-1}$) (**8b**), 364 nm ($10\,832\text{ M}^{-1}\text{ cm}^{-1}$) (**8c**), 360 nm ($12\,341\text{ M}^{-1}\text{ cm}^{-1}$) (**9b**), 362 nm ($13\,830\text{ M}^{-1}\text{ cm}^{-1}$) (**9c**). The π – π^* transition band decreased in intensity after photoirradiation, indicating the photoisomerization of the *trans* form to the *cis* form (*trans*-to-*cis*) [10,31]. The reverse process, a *cis*-to-*trans* change is

observed under thermal conditions (*vide supra*). Perfect recovery of the *trans* form is not achieved either by photoirradiation or by a thermal reaction process, which indicates either permanent photochemical change or irreversible phototransformation to some unidentified product(s). The later possibility may be discouraged as the spectral pattern remains unchanged even after 10 h visible light exposure. We do not rule out the possibility of coordination of solvent (CH₃CN) to copper(I) upon light irradiation. The complexes [Cu(SMeaaiNH)(PPh₃)Cl] (**4a**), [Cu(SEtaaiNH)(PPh₃)Cl] (**5a**), [Cu(SMeaaiNH)(PPh₃)Br] (**6a**), [Cu(SEtaaiNH)(PPh₃)Br] (**7a**), [Cu(SMeaaiNH)(PPh₃)I] (**8a**) and [Cu(SEtaaiNH)(PPh₃)I] (**9a**) do not exhibit photochromism under identical conditions. The metal ion and its oxidation state, nature of the ligand, presence of other coordinating ligand(s), etc. play an important role in the photoisomerization of the coordinated ligand in the complexes [32–35]. It is proposed that UV-light irradiation may cleave the Cu–N(azo) bond to make a free rotatory azo-aryl group which isomerizes to the *cis*-form. Because of the long Cu(1)–N(azo) distance (*vide supra*), the molecule may exhibit photophysical activation *via* cleavage of this bond followed by rotation to introduce photoisomerization. The quantum yields were measured for the *trans*-to-*cis* ($\phi_{t\rightarrow c}$)

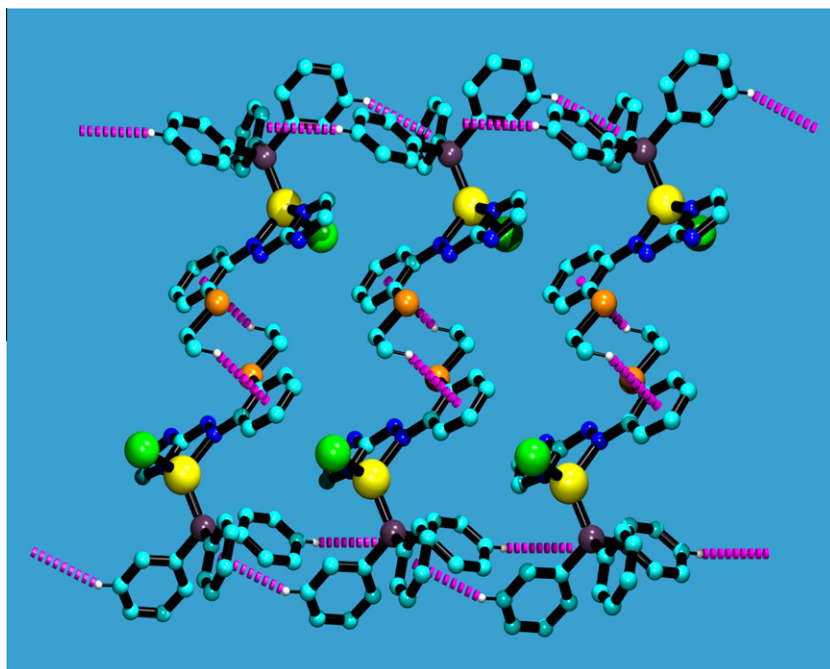


Fig. 4. C–H... π and π – π stacked 2D diagram of [Cu(SEtaaiNH)(PPh₃)I] (**9a**).

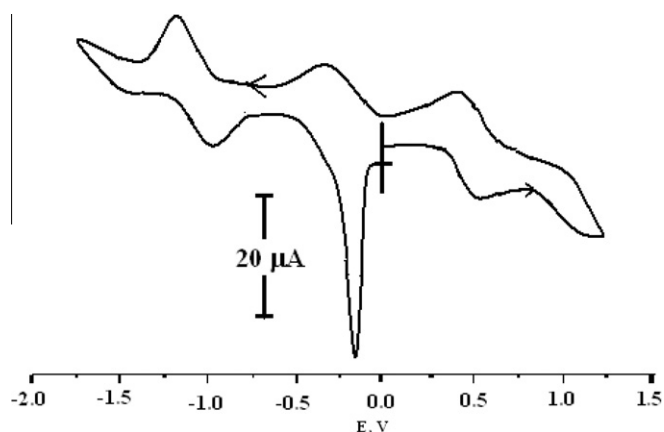


Fig. 5. Cyclic voltammogram of [Cu(SEtaaiNEt)(PPh₃)Cl] (**5c**) in MeCN.

photoisomerization of these compounds in MeCN on irradiation with UV wavelength light (Supplementary Material, Table S4). In general, an increase in the mass of a molecule reduces the rate of isomerization, *trans*-to-*cis* [32,36,37]. In the complexes, the $\phi_{\tau \rightarrow c}$ values are significantly less than that of the free ligand data [38].

Thermal *cis*-to-*trans* isomerization of the ligands and complexes were followed by UV–Vis spectroscopy in MeCN at various temperatures, 298–313 K. The Eyring plots (Fig. 7) in the range 298–313 K gave a linear graph, from which the activation energy is obtained (Supplementary Material, Table S5). In the complexes, the E_a values are severely reduced, which means faster *cis*-to-*trans* thermal isomerization of the complexes. The entropies of activation (ΔS^\ddagger) are more negative in the complexes than that of the free ligand. This is also in support of an increase in the rotor volume of the complexes.

2.6. Electronic structure of [Cu(SEtaaiNH)(PPh₃)I] (**9a**)

Density functional theory (DFT) calculations have been useful to describe the electronic configuration, physical, chemical, catalytic

properties, predicting the reaction mechanism and redox properties of complex compounds, bio-molecules, etc. The DFT calculations of [Cu(SEtaaiNH)(PPh₃)I] (**9a**) have been performed using the GAUSSIAN 03 analyses package. Structural agreement has been observed from a comparison of bond distances and angles between the calculated and X-ray determined structures (Table 1). The orbital energies, along with contributions from the ligands and metal, are given as Supplementary material, and Fig. 8 depicts selected occupied and unoccupied frontier orbitals in the gas phase calculation. The highest occupied molecular orbital (HOMO) (energy -4.38 eV) is dominated by I character (85%), while Cu contributes only 12%. HOMO -1 (-4.48 eV) also bears 81% character from the I group, while HOMO -2 , HOMO -3 , etc. are dominated by functions of Cu ($>50\%$). The LUMO (lowest unoccupied MO, -2.70 eV) has 90% characteristics of SEtaaiNH, in which the azo group shares a half portion (45%). LUMO $+1$, LUMO $+2$ and LUMO $+3$ are dominated by ($>75\%$) functions from PPh₃. The calculated transitions are grouped in Table 2. The intensity of these transitions has been assessed from the oscillator strength (f). The band at 687 nm (f , 0.0746) is an admixture of MLCT and $I \rightarrow \pi^*(\text{SEtaaiNH})$ transition, while 427 nm (f , 0.1162), an intense band, is defined as a $\pi(\text{SEtaaiNH}) \rightarrow \pi^*(\text{SEtaaiNH})$ transition. A significant transition at 337 nm (f , 0.013) is assigned to a MLCT ($d(\text{Cu}) \rightarrow \pi^*(\text{SEtaaiNH})$) transition. An intense band at 331 nm (f , 0.1153) is also an admixture of $I \rightarrow \pi^*(\text{SEtaaiNH})$ and $I \rightarrow \pi^*(\text{PPh}_3)$ transitions, while bands at 329 and 326 nm are assigned to $\pi(\text{PPh}_3) \rightarrow \pi^*(\text{SEtaaiNH})$ transitions. Other transitions in the UV region are mainly due to ligand to ligand charge transfer transitions. Thus, the excitation may lead to charge population at the chelated SEtaaiNH dominated function, that may be manifested by cleavage of the longer bond, Cu–N(azo), followed by immediate rotation about the $-\text{N}=\text{N}-$ bond. This may lead to *trans*-to-*cis* isomerization. This is indeed observed.

The cyclic voltammetric behavior of the complexes is readily accountable from the DFT calculations. Because of the higher metal (Cu) function in the occupied MOs, the complexes show a metal oxidation Cu(II)/Cu(I) couple. The unoccupied MOs are significantly dominated by the azoimine function, thus reduction may refer to

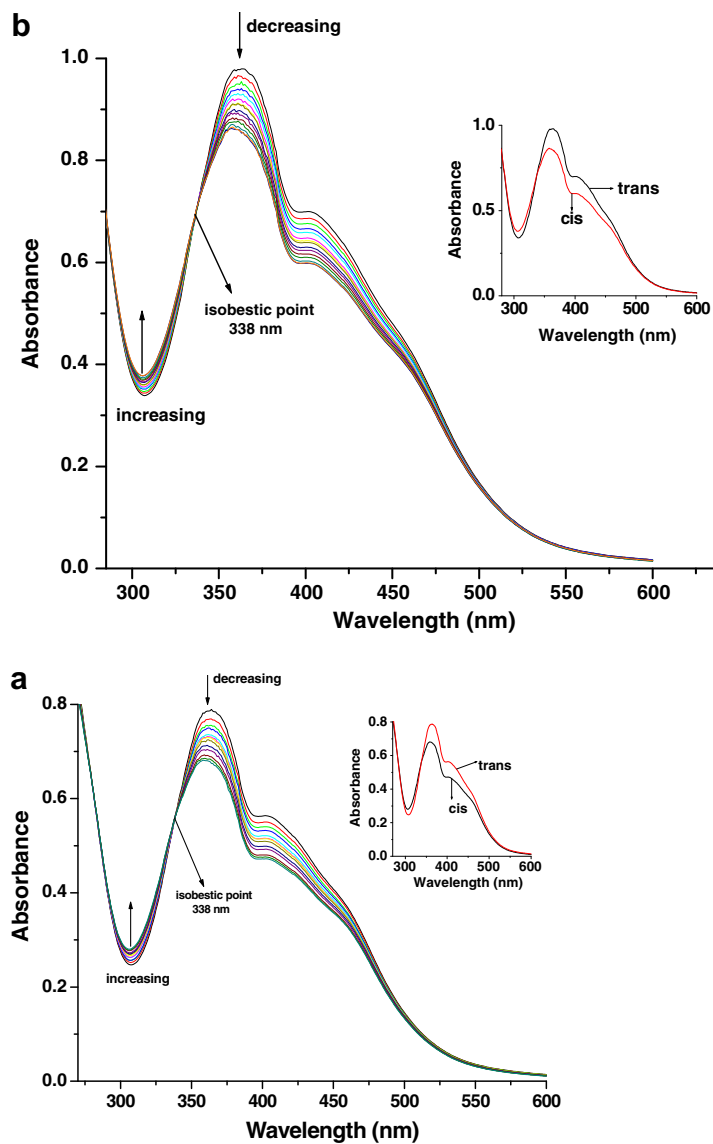
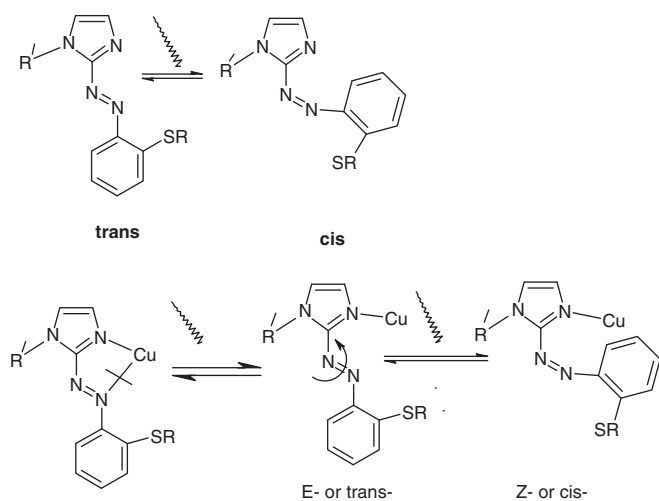


Fig. 6. Spectral changes of (a) [Cu(SMeaaiNEt)(PPh₃)Cl] (**4c**) (irradiation at 361 nm) and (b) [Cu(SEtaaiNMe)(PPh₃)Cl] (**5b**) (irradiation at 357 nm) at 6 min interval at 25 °C in acetonitrile. Inset figure shows spectra of the *cis* and *trans* isomers of the complex.



Scheme 2. Photochromism of free and coordinated SRaaiNR.

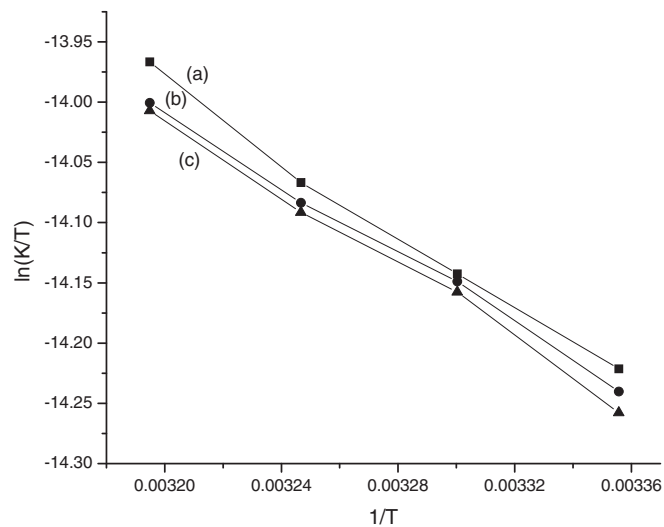


Fig. 7. Eyring plots of Z-to-E thermal isomerization of (a) [Cu(SMeaaiNEt)(PPh₃)Cl] (**4c**), (b) [Cu(SMeaaiNEt)(PPh₃)Br] (**6c**) and (c) [Cu(SMeaaiNEt)(PPh₃)Br] (**8c**) at different temperatures.

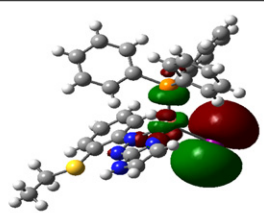
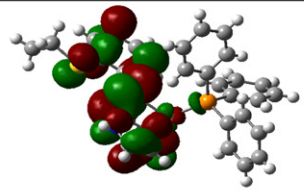
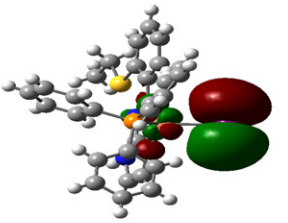
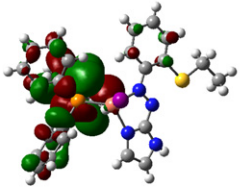
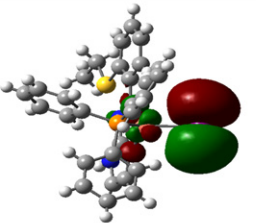
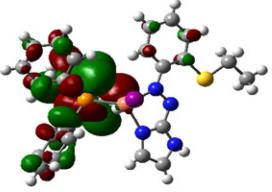
HOMO	LUMO
 <p>E = - 4.38 eV; Cu, 12%; I, 81%; PPh₃, 5%; SEtaaiNH, 2%</p>	 <p>E = - 2.70 eV; Cu, 5%; I, 3%; PPh₃, 2%; SEtaaiNH, 90%</p>
HOMO - 1	LUMO + 1
 <p>E = - 4.48 eV; Cu, 12%; I, 85%; SEtaaiNH, 3%</p>	 <p>E = - 0.65 eV; PPh₃, 96%; SEtaaiNH, 3%</p>
HOMO - 2	LUMO + 2
 <p>E = - 4.87 eV; Cu, 29%; I, 55%; PPh₃, 5%; SEtaaiNH, 11%</p>	 <p>E = - 0.50 eV; PPh₃, 96%; SEtaaiNH, 4%</p>

Fig. 8. Contour plots of some MOs with their energy and composition for [Cu(SEtaaiNH)(PPh₃)] (**9a**).

electron accommodation at the azo dominated orbital of the ligand. So the assignment of azo reductions is justified.

Table 2
Selected list of transitions obtained from TD-DFT calculations in the gas phase of [Cu(SEtaaiNH)(PPh₃)] (**9a**).

Excited state	Wavelength (nm)	Oscillator strength	Transitions	Assignment
3	687	0.0746	(61%) H - 2 → L	XLCT(Major) + MLCT
6	427	0.1162	(63%) H - 5 → L	ILCT
18	337	0.0130	(39%) H - 11 → L (21%) H - 12 → L	YLCT(Major)+MLCT MLCT(Major)+XLCT
21	331	0.1153	(56%) H - 1 → L + 4	XLCT + XYCT
22	329	0.0104	(66%) H - 10 → L (12%) H - 8 → L	YLCT YLCT
23	326	0.0184	(41%) H - 11 → L (15%) H → L + 6	YLCT(Major)+MLCT XLCT
40	285	0.0136	(54%) H - 2 → L + 5	XYCT + MYCT
44	275	0.0358	(64%) H - 3 → L + 1 (23%) H - 2 → L + 8	MYCT + MYCT
46	268	0.0157	(66%) H - 2 → L + 9	XLCT + MLCT
47	266	0.0128	(68%) H - 3 → L + 2	MYCT
50	261	0.0379	(67%) H - 3 → L + 3 (11%) H - 4 → L + 3	MYCT + YLCT + MLCT

3. Experimental

Materials: Imidazole, different aromatic amines, CuX (X = Cl, Br, I) and triphenyl phosphine were purchased from E. Merck India. All other chemicals and solvents were of reagent grade and used as received. 1-Alkyl-2-(arylo)imidazoles (RaaiR') were prepared by a reported procedure [39]. The syntheses of the ligands were carried out following the coupling of the *o*-(thioalkyl)phenyldiazonium ion (obtained by diazotization of *o*-(thioalkyl)aniline) with imidazole at pH 7, followed by N(1)-alkylation using alkyl iodide in the presence of NaH in dry THF under dry and inert conditions [26].

3.1. Physical measurements

Microanalytical data (C, H, N) were collected on a Perkin-Elmer 2400 CHNS/O elemental analyzer. Spectroscopic data were obtained using the following instruments: UV-Vis spectra, Perkin-Elmer; model Lambda 25; IR spectra (KBr disk, 4000–450 cm⁻¹), Perkin-Elmer; model RX-1; ¹H NMR spectra, Bruker (AC) 300 MHz FTNMR spectrometer. Electrochemical measurements were performed using a computer-controlled PAR model 250 VersaStat electrochemical instruments with Pt-disk electrodes. All

Table 3
Summarized crystallographic data for [Cu(SEtaaiNH)(PPh₃)I] (**9a**).

Empirical formula	C ₂₉ H ₂₆ N ₄ PSiCu
Formula weight	685.01
T (K)	298(2)
Crystal size (mm)	0.16 × 0.14 × 0.12
Crystal system	triclinic
Space group	P1̄
a (Å)	8.2050(2)
b (Å)	9.5070(3)
c (Å)	21.7100(7)
α (°)	89.447(2)
β (°)	84.103(2)
γ (°)	66.357(2)
V (Å ³)	1542.21(8)
Radiation (λ, Å)	1.54184
Z	2
μ (Cu Kα) (mm ⁻¹)	10.159
θ Range for data collection (°)	4.10–73.38
Index ranges	−10 ≤ h ≤ 10, −11 ≤ k ≤ 11, −13 ≤ l ≤ 26
D _{calc} (Mg m ⁻³)	1.473
Refine parameters	335
F(0 0 0)	682
Total reflections	6334
Unique reflections	5289
R ₁ ^a [I > 2σ(I)]	0.0580
wR ₂ ^b	0.1456
Goodness of fit	1.116
Largest difference in peak and hole (e Å ⁻³)	−0.713 and 0.777

$$^a R = \sum |F_o| - |F_c| / \sum |F_o|$$

$$^b wR_2 = \left[\frac{\sum w(F_o^2 - F_c^2)^2}{\sum w(F_o^2)^2} \right]^{1/2}, \quad wR_2 = \left[\frac{\sum w(F_o^2 - F_c^2)^2}{\sum w(F_o^2)^2} \right]^{1/2},$$

$$w = 1 / [\sigma^2(F_o^2) + (0.0484P)^2 + (3.4781P)], \text{ where } P = (F_o^2 + 2F_c^2) / 3.$$

measurements were carried out under a nitrogen environment at 298 K with reference to SCE in acetonitrile, using [nBu₄N][ClO₄] as a supporting electrolyte. The reported potentials are uncorrected for junction potential. Room temperature (298 K) magnetic susceptibility was measured using Sherwood Scientific Cambridge, UK at 298 K.

3.2. Synthesis of complexes

3.2.1. [Cu(SEtaaiNH)(PPh₃)I] (**9a**)

1-Methyl-2-[o-(thiomethyl)phenylazo]imidazole (SMeaiiNMe) (200 mg, 0.86 mmol) in methanol (10 ml) was added dropwise to a methanolic solution (10 ml) of CuI (112 mg, 0.88 mmol), followed by the addition of PPh₃ (236 mg, 0.9 mmol) at 298 K. The brown-red solution was stirred for 10 min. The resulting solution was then refluxed for 3 h. It was then filtered and left undisturbed for a week. Dark brown crystalline compounds separated out. The crystals were filtered, washed with water, cold methanol and dried *in vacuo*. The yield was 368 mg (67%).

All the other complexes were prepared by the same procedure. The yields varied from 60% to 75% and microanalytical and spectral data of the complexes are given herewith.

Anal. Calc. for [Cu(SMeaiiNH)(PPh₃)Cl] (**4a**), C₂₈H₂₅CuN₄PSiCl: C, 58.08; H, 4.35; N, 9.67. Found: C, 58.12; H, 4.44; N, 9.59%. FT-IR (KBr disc, cm⁻¹): ν(N–H), 3007; ν(N=N), 1430; ν(C=N), 1597. UV–Vis spectral data in CH₃CN (λ_{max} (nm) (10⁻³ ε (dm³ mol⁻¹ cm⁻¹)): 606 (0.43), 459 (6.37), 411 (8.93), 358 (15.58), 254(24.91). *Anal. Calc.* for [Cu(SMeaiiNMe)(PPh₃)Cl] (**4b**), C₂₉H₂₇CuN₄PSiCl: C, 58.68; H, 4.91; N, 9.44. Found: C, 58.79; H, 4.97; N, 9.34%. FT-IR (KBr disc, cm⁻¹): ν(N=N), 1429; ν(C=N), 1583. UV–Vis spectral data in CH₃CN (λ_{max} (nm) (10⁻³ ε (dm³ mol⁻¹ cm⁻¹)): 602 (1.15), 468 (6.39), 417 (11.32), 364 (14.53), 262 (21.54). *Anal. Calc.* for [Cu(SMeaiiNEt)(PPh₃)Cl] (**4c**), C₃₀H₂₉CuN₄PSiCl: C, 59.30; H, 4.81; N, 9.22. Found: C, 59.46; H,

4.79; N, 9.28%. FT-IR (KBr disc, cm⁻¹): ν(N=N), 1425; ν(C=N), 1591. UV–Vis spectral data in CH₃CN (λ_{max} (nm) (10⁻³ ε (dm³ mol⁻¹ cm⁻¹)): 623 (0.73), 456 (5.24), 405 (8.09), 361 (11.42), 259 (15.17). *Anal. Calc.* for [Cu(SEtaaiNH)(PPh₃)Cl] (**5a**), C₂₉H₂₇CuN₄PSiCl: C, 58.68; H, 4.91; N, 9.44. Found: C, 58.79; H, 4.88; N, 9.38%. FT-IR (KBr disc, cm⁻¹): ν(N=N), 1432; ν(C=N), 1587. UV–Vis spectral data in CH₃CN (λ_{max} (nm) (10⁻³ ε (dm³ mol⁻¹ cm⁻¹)): 612 (0.32), 455 (5.15), 417 (9.49), 363 (12.25), 251 (20.53). *Anal. Calc.* for [Cu(SEtaaiNMe)(PPh₃)Cl] (**5b**), C₃₀H₂₉CuN₄PSiCl: C, 59.30; H, 4.81; N, 9.22. Found: C, 59.44; H, 4.84; N, 9.29%. FT-IR (KBr disc, cm⁻¹): ν(N=N), 1424; ν(C=N), 1584. UV–Vis spectral data in CH₃CN (λ_{max} (nm) (10⁻³ ε (dm³ mol⁻¹ cm⁻¹)): 617 (0.61), 462 (3.39), 403 (5.89), 357 (8.84), 259 (12.88). *Anal. Calc.* for [Cu(SEtaaiNEt)(PPh₃)Cl] (**5c**), C₃₁H₃₁CuN₄PSiCl: C, 59.81; H, 5.02; N, 8.99. Found: C, 59.89; H, 5.09; N, 8.78%. FT-IR (KBr disc, cm⁻¹): ν(N=N), 1418; ν(C=N), 1591. UV–Vis spectral data in CH₃CN (λ_{max} (nm) (10⁻³ ε (dm³ mol⁻¹ cm⁻¹)): 608 (0.83), 465 (11.23), 420 (14.43), 365 (18.95), 252 (27.32). *Anal. Calc.* for [Cu(SMeaiiNH)(PPh₃)Br] (**6a**), C₂₈H₂₅CuN₄PSiBr: C, 53.89; H, 4.04; N, 9.02. Found: C, 53.78; H, 4.06; N, 9.08%. FT-IR (KBr disc, cm⁻¹): ν(N=N), 1428; ν(C=N), 1582. UV–Vis spectral data in CH₃CN (λ_{max} (nm) (10⁻³ ε (dm³ mol⁻¹ cm⁻¹)): 600 (0.54), 460 (7.46), 411 (10.31), 359 (13.51), 242 (21.24). *Anal. Calc.* for [Cu(SMeaiiNMe)(PPh₃)Br] (**6b**), C₂₉H₂₇CuN₄PSiBr: C, 54.59; H, 4.27; N, 8.78. Found: C, 54.51; H, 4.29; N, 8.87%. FT-IR (KBr disc, cm⁻¹): ν(N=N), 1422; ν(C=N), 1586. UV–Vis spectral data in CH₃CN (λ_{max} (nm) (10⁻³ ε (dm³ mol⁻¹ cm⁻¹)): 598 (0.29), 455 (4.98), 402 (9.32), 358 (12.22), 249 (19.32). *Anal. Calc.* for [Cu(SMeaiiNEt)(PPh₃)Br] (**6c**), C₃₀H₂₉CuN₄PSiBr: C, 55.26; H, 4.48; N, 8.52. Found: C, 55.38; H, 4.43; N, 8.59%. FT-IR (KBr disc, cm⁻¹): ν(N=N), 1429; ν(C=N), 1581. UV–Vis spectral data in CH₃CN (λ_{max} (nm) (10⁻³ ε (dm³ mol⁻¹ cm⁻¹)): 621 (0.59), 451 (7.84), 405 (9.43), 363 (13.48), 261 (21.78). *Anal. Calc.* for [Cu(SEtaaiNH)(PPh₃)Br] (**7a**), C₂₉H₂₇CuN₄PSiBr: C, 54.59; H, 4.27; N, 8.78. Found: C, 54.53; H, 4.28; N, 8.83%. FT-IR (KBr disc, cm⁻¹): ν(N=N), 1415; ν(C=N), 1593. UV–Vis spectral data in CH₃CN (λ_{max} (nm) (10⁻³ ε (dm³ mol⁻¹ cm⁻¹)): 601 (1.23), 457 (4.34), 402 (8.43), 360 (12.65), 252 (25.67). *Anal. Calc.* for [Cu(SEtaaiNMe)(PPh₃)Br] (**7b**), C₃₀H₂₉CuN₄PSiBr: C, 55.26; H, 4.48; N, 8.52. Found: C, 55.35; H, 4.42; N, 8.55%. FT-IR (KBr disc, cm⁻¹): ν(N=N), 1417; ν(C=N), 1584. UV–Vis spectral data in CH₃CN (λ_{max} (nm) (10⁻³ ε (dm³ mol⁻¹ cm⁻¹)): 601 (0.68), 462 (5.32), 415 (9.54), 361 (11.93), 249 (26.41). *Anal. Calc.* for [Cu(SEtaaiNEt)(PPh₃)Br] (**7c**), C₃₁H₃₁CuN₄PSiBr: C, 55.82; H, 4.68; N, 8.40. Found: C, 55.91; H, 4.65; N, 8.31%. FT-IR (KBr disc, cm⁻¹): ν(N=N), 1421; ν(C=N), 1580. UV–Vis spectral data in CH₃CN (λ_{max} (nm) (10⁻³ ε (dm³ mol⁻¹ cm⁻¹)): 621 (0.64), 459 (5.63), 406 (8.48), 363 (13.48), 260 (22.32). *Anal. Calc.* for [Cu(SMeaiiNH)(PPh₃)I] (**8a**), C₂₈H₂₅CuN₄PSiI: C, 50.12; H, 3.76; N, 8.35. Found: C, 50.22; H, 3.75; N, 8.31%. FT-IR (KBr disc, cm⁻¹): ν(N=N), 1427; ν(C=N), 1587. UV–Vis spectral data in CH₃CN (λ_{max} (nm) (10⁻³ ε (dm³ mol⁻¹ cm⁻¹)): 618 (0.71), 465 (5.31), 416 (9.48), 366 (13.12), 254 (26.54). *Anal. Calc.* for [Cu(SMeaiiNMe)(PPh₃)I] (**8b**), C₂₉H₂₇CuN₄PSiI: C, 50.85; H, 3.97; N, 8.12. Found: C, 50.71; H, 3.99; N, 8.17%. FT-IR (KBr disc, cm⁻¹): ν(N=N), 1428; ν(C=N), 1590. UV–Vis spectral data in CH₃CN (λ_{max} (nm) (10⁻³ ε (dm³ mol⁻¹ cm⁻¹)): 610 (0.74), 460 (4.48), 400 (7.90), 363 (13.83), 244 (19.48). *Anal. Calc.* for [Cu(SMeaiiNEt)(PPh₃)I] (**8c**), C₃₀H₂₉CuN₄PSiI: C, 51.54; H, 4.18; N, 8.01. Found: C, 51.65; H, 4.16; N, 8.08%. FT-IR (KBr disc, cm⁻¹): ν(N=N), 1431; ν(C=N), 1589. UV–Vis spectral data in CH₃CN (λ_{max} (nm) (10⁻³ ε (dm³ mol⁻¹ cm⁻¹)): 609 (0.51), 463 (5.75), 405 (9.46), 364 (10.83), 243 (23.48). *Anal. Calc.* for [Cu(SEtaaiNH)(PPh₃)I] (**9a**), C₂₉H₂₇CuN₄PSiI: C, 50.85; H, 3.97; N, 8.12. Found: C, 50.78; H, 3.94; N, 8.15%. FT-IR (KBr disc, cm⁻¹): ν(N=N), 1422; ν(C=N),

1592. UV–Vis spectral data in CH₃CN (λ_{max} (nm) ($10^{-3} \epsilon$ (dm³ mol⁻¹ cm⁻¹)): 601 (1.32), 458 (10.32), 403 (14.46), 361 (19.43), 249 (31.43). *Anal. Calc.* for [Cu(SEtaaiNMe)(PPh₃)I] (**9b**), C₃₀H₂₉CuN₄PSI: C, 51.54; H, 4.18; N, 8.01. Found: C, 51.62; H, 4.20; N, 8.10%. FT-IR (KBr disc, cm⁻¹): $\nu(\text{N}=\text{N})$, 1418; $\nu(\text{C}=\text{N})$, 1595. UV–Vis spectral data in CH₃CN (λ_{max} (nm) ($10^{-3} \epsilon$ (dm³ mol⁻¹ cm⁻¹)): 611 (0.23), 463 (5.42), 412 (9.32), 360 (12.34), 251 (22.54). *Anal. Calc.* for [Cu(SEtaaiNEt)(PPh₃)I] (**9c**), C₃₁H₃₁CuN₄PSI: C, 52.15; H, 4.38; N, 7.85. Found: C, 52.24; H, 4.34; N, 7.89%. FT-IR (KBr disc, cm⁻¹): $\nu(\text{N}=\text{N})$, 1412; $\nu(\text{C}=\text{N})$, 1587. UV–Vis spectral data in CH₃CN (λ_{max} (nm) ($10^{-3} \epsilon$ (dm³ mol⁻¹ cm⁻¹)): 603 (0.59), 461 (5.40), 409 (9.41), 362 (13.83), 245 (27.84).

3.3. X-ray crystal structure analysis of [Cu(SEtaaiNH)(PPh₃)I] (**9a**)

Details of the crystal analyses, data collection and structure refinement data are given in Table 3. Single crystal data collections were performed with a Siemens SMART CCD diffractometer using fine focus sealed graphite-monochromatized Cu K α radiation. Data were corrected for Lorentz polarization effects and for linear decay. Semi-empirical absorption corrections based on ω -scans were applied. The structure was solved by direct methods using SHELXS-97 and successive difference Fourier syntheses [40]. All non-hydrogen atoms were refined anisotropically. The hydrogen atoms were fixed geometrically and refined using the riding model. The final difference Fourier map of residual electron density was carried out using SHELXL-97 [41]. The structures were drawn using ORTEP-32 [42] and PLATON-99 [43] programs.

3.4. Photometric measurements

Absorption spectra were taken with a Perkin–Elmer Lambda 25 UV–Vis spectrophotometer in a 1 × 1 cm quartz optical cell maintained at 25 °C with a Peltier thermostat. The light source of a Perkin–Elmer LS 55 spectrofluorimeter was used as the excitation light, with a slit width of 10 nm. An optical filter was used to cut off overtones when necessary. The absorption spectra of the *cis* isomers were obtained by extrapolation of the absorption spectra of a *cis*-rich mixture, for which the composition is known from ¹H NMR integration. Quantum yields (ϕ) were obtained by measuring initial *trans*-to-*cis* isomerization rates (ν) in a well-stirred solution within the above instrument using the equation:

$$\nu = (\phi I_0 / V)(1 - 10^{-\text{Abs}})$$

where I_0 is the photon flux at the front of the cell, V is the volume of the solution, and Abs is the initial absorbance at the irradiation wavelength. The value of I_0 was obtained using azobenzene ($\phi = 0.11$ for a π - π^* excitation [44]) under the same irradiation conditions.

The thermal *cis*-to-*trans* isomerization rates were obtained by monitoring absorption changes intermittently for a *cis*-rich solution kept in the dark at constant temperatures (T) in the range 298–313 K. The activation energy (E_a) and the frequency factor (A) were obtained from the Eyring plot:

$$\ln k/T = \ln A - E_a/RT$$

where k is the measured rate constant, R is the gas constant and T is temperature. The values of the activation free energy (ΔG^\ddagger) and activation entropy (ΔS^\ddagger) were obtained through the relationships,

$$\Delta G^\ddagger = E_a - RT - T\Delta S^\ddagger \quad \text{and} \quad \Delta S^\ddagger = [\ln A - 1 - \ln(kBT/h)]/R$$

where k_B and h are Boltzmann's and Planck's constants, respectively

3.5. Computational methods

The density functional theory (DFT) calculations on the crystal structure of [Cu(SEtaaiNH)(PPh₃)I] (**9a**) was carried out using the GAUSSIAN 03w program package [45], with the aid of the GAUSSVIEW visualization program [46]. The hybrid functional by Becke, B3LYP [45], was used, which includes a mixture of Hartree–Fock exchange with DFT exchange–correlation. For C, H, N, and I, we used MIDI1 basis functions [48] as this basis set is applicable to all these elements and includes polarization functions. For Cu, we used the LanL2DZ basis set, including Los Alamos Effective Core Potentials [49–51].

4. Conclusion

1-Alkyl-2- $\{(o\text{-thioalkyl})\text{phenylazo}\}$ imidazole (SRaaiNR') acts as a bidentate N(imidazole), N(azo) chelator to a Cu(I) center. The reaction of CuX and PPh₃ followed by the addition of SRaaiNR' isolated complexes of the composition [Cu(SRaaiNR')(PPh₃)X] (X = Cl, Br, I). One of the complexes was structurally characterized by a single crystal X-ray diffraction study. The complexes show *trans*-to-*cis* isomerization of the coordinated azoimidazole upon light irradiation in the UV range. Quantum yields ($\phi_{t \rightarrow c}$) of photoisomerization were calculated, and the free ligand shows a higher ϕ value than the Cu(I) complexes. The *cis*-to-*trans* isomerization is a thermally induced process. The activation energy (E_a) of the *cis*-to-*trans* isomerization was calculated by a controlled temperature experiment. DFT calculations determine the electronic structure and explain the spectra and cyclic voltammetric properties of the complexes.

Acknowledgment

Financial support from Department of Science and Technology, New Delhi is gratefully acknowledged.

Appendix A. Supplementary data

CCDC 792771 contains the supplementary crystallographic data for [Cu(SEtaaiNH)(PPh₃)I]. These data can be obtained free of charge via <http://www.ccdc.cam.ac.uk/conts/retrieving.html>, or from the Cambridge Crystallographic Data Centre, 12 Union Road, Cambridge CB2 1EZ, UK; fax: (+44) 1223-336-033; or e-mail: deposit@ccdc.cam.ac.uk. Supplementary data associated with this article can be found, in the online version, at [doi:10.1016/j.poly.2010.11.036](https://doi.org/10.1016/j.poly.2010.11.036).

References

- [1] H. Rau, in: H. Dürr, H. Bounas-Laurent (Eds.), *Photochromism Molecules and Systems*, Elsevier, Amsterdam, 1990, p. 165.
- [2] N. Tamai, H. Miyasaka, *Chem. Rev.* 100 (2000) 1857.
- [3] H. Sugimoto, *CRC Handbook of Organic Photochemistry and Photobiology*, 2nd ed., CRC Press, Boca Raton, FL, 2004 (Chapter 94).
- [4] B.L. Feringa (Ed.), *Molecular Switches*, Wiley–VCH, Weinheim, 2001.
- [5] S. Yagai, T. Karatsu, A. Kitamura, *Chem. Eur. J.* 11 (2005) 4054.
- [6] S. Yagai, T. Nakajima, T. Karatsu, K. Saitow, A. Kitamura, *J. Am. Chem. Soc.* 126 (2004) 11500.
- [7] E. Markava, D. Gustina, I. Muzikante, L. Gerca, M. Rutkis, E. Fonavs, *Mol. Cryst. Liq. Cryst.* 355 (2001) 381.
- [8] D. Datta, A. Chakravorty, *Inorg. Chem.* 22 (1983) 1085.
- [9] P.K. Santra, D. Das, T.K. Misra, R. Roy, C. Sinha, S.-M. Peng, *Polyhedron* 18 (1999) 1909.
- [10] J. Otsuki, K. Suwa, K. Narutaki, C. Sinha, I. Yoshikawa, K. Araki, *J. Phys. Chem. A* 109 (2005) 8064.
- [11] J. Otsuki, K. Suwa, K.K. Sarker, C. Sinha, *J. Phys. Chem. A* 111 (2007) 1403.
- [12] V.K. Ahluwalia, B. Mittal, R.P. Singh Ra, P. Singh, R.R. Mann, S.B. Singh, *Indian J. Chem.* 28B (1989) 150.
- [13] J. Otsuki, K. Narutaki, *Bull. Chem. Soc. Jpn.* 77 (2004) 1537.
- [14] J. Otsuki, K. Narutaki, J.M. Bakke, *Chem. Lett.* 33 (2004) 356.
- [15] B.G. Chand, U. Ray, G. Mostafa, T.-H. Lu, C. Sinha, *J. Coord. Chem.* 57 (2004) 627.
- [16] U. Ray, D. Banerjee, G. Mostafa, T.-H. Lu, C. Sinha, *New J. Chem.* 28 (2004) 1437.

- [17] J. Dinda, S. Jasimuddin, G. Mostafa, C.-H. Hung, C. Sinha, *Polyhedron* 23 (2004) 793.
- [18] S. Jasimuddin, C. Sinha, *Transition Met. Chem.* 29 (2004) 566.
- [19] B.G. Chand, U.S. Ray, G. Mostafa, J. Cheng, T.-H. Lu, C. Sinha, *Inorg. Chim. Acta* 358 (2005) 1927.
- [20] S.S.S. Raj, H.-K. Fun, X.-F. Chen, X.-H. Zhu, X.-Z. You, *Acta Crystallogr., Sect. C* 55 (1999) 1644.
- [21] A.C. Dash, A. Acharya, R.K. Sahoo, *Indian J. Chem.* 37A (1998) 759.
- [22] M.N. Ackermann, M.P. Robinson, I.A. Maher, E.B. LeBlanc, R.V. Raz, *J. Organomet. Chem.* 682 (2003) 248.
- [23] K.K. Sarker, B.G. Chand, K. Suwa, J. Cheng, T.-H. Lu, J. Otsuki, C. Sinha, *Inorg. Chem.* 46 (2007) 670.
- [24] K.K. Sarker, D. Sardar, K. Suwa, J. Otsuki, C. Sinha, *Inorg. Chem.* 46 (2007) 8291.
- [25] P. Pratihari, T.K. Mondal, A.K. Patra, C. Sinha, *Inorg. Chem.* 48 (2009) 2760.
- [26] D. Banerjee, U.S. Ray, S.K. Jasimuddin, J.-C. Liou, T.-H. Lu, C. Sinha, *Polyhedron* 25 (2006) 1299.
- [27] M.K. Casida, in: D.P. Chong (Ed.), *Recent Advances in Density Functional Methods, Part I*, World Scientific, Singapore, 1995.
- [28] M. Petersilka, U.J. Gossmann, E.K.U. Gross, *Phys. Rev. Lett.* 76 (1996) 1212.
- [29] G. Saha, K.K. Sarker, P. Datta, P. Raghavaiah, C. Sinha, *Polyhedron* 29 (2010) 2098.
- [30] J. Dinda, U.S. Ray, G. Mostafa, T.-H. Lu, A. Usman, I. Abdul Razak, S. Chantrapromma, H.-K. Fun, C. Sinha, *Polyhedron* 22 (2003) 247.
- [31] J. Otsuki, K. Suwa, K.K. Sarker, C. Sinha, *J. Phys. Chem. A* 111 (2007) 1403.
- [32] H. Nishihara, *Bull. Chem. Soc. Jpn.* 77 (2004) 407.
- [33] D.J. Fitzmaurice, M. Esche, H. Frei, J. Moser, *J. Phys. Chem.* 97 (1993) 3806.
- [34] A.T. Hutton, H.M.N.H. Irving, *J. Chem. Soc., Dalton Trans.* (1982) 2299.
- [35] G. Zentai, L. Partain, R. Pavlyuchkova, C. Proano, G. Virshup, L. Melekshov, A. Zuck, B.N. Breen, O. Dagan, A. Vilensky, M. Schieber, H. Gilboa, P. Bennet, K. Shah, Y. Dimitriev, J. Thomas, M. Yaffe, D. Hunter, D. Proc. SPIE MI (2003) 5030.
- [36] T. Yutaka, M. Kurihara, H. Nishihara, *Mol. Cryst. Liq. Cryst.* 343 (2000) 193.
- [37] T. Yutaka, L. Mori, M. Kurihara, J. Mizutani, K. Kubo, S. Furusho, K. Matsumura, N. Tamai, H. Nishihara, *Inorg. Chem.* 40 (2001) 4986.
- [38] K.K. Sarker, S. Saha Halder, D. Banerjee, T.K. Mondal, A.R. Paital, P.K. Nanda, P. Raghavaiah, C. Sinha, *Inorg. Chim. Acta* 363 (2010) 2955.
- [39] T.K. Misra, D. Das, C. Sinha, P.K. Ghosh, C.K. Pal, *Inorg. Chem.* 37 (1998) 1672.
- [40] G.M. Sheldrick, *SHELXS-97*, Program for the Solution of Crystal Structures, University of Göttingen, Germany, 1997.
- [41] G.M. Sheldrick, *SHELXL 97*, Program for the Refinement of Crystal Structures, University of Göttingen, Germany, 1997.
- [42] L.J. Farrugia, *J. Appl. Cryst.* 30 (1997) 565.
- [43] A.L. Spek, *PLATON*, Molecular Geometry Program, University of Utrecht, The Netherlands, 1999.
- [44] G. Zimmerman, L. Chow, U. Paik, *J. Am. Chem. Soc.* 80 (1958) 3528.
- [45] M.J. Frisch, G.W. Trucks, H.B. Schlegel, G.E. Scuseria, M.A. Robb, J.R. Cheeseman, J.A. Montgomery Jr., T. Vreven, K.N. Kudin, J.C. Burant, J.M. Millam, S.S. Iyengar, J. Tomasi, V. Barone, B. Mennucci, M. Cossi, G. Scalmani, N. Rega, G.A. Petersson, H. Nakatsuji, M. Hada, M. Ehara, K. Toyota, R. Fukuda, J. Hasegawa, M. Ishida, T. Nakajima, Y. Honda, O. Kitao, H. Nakai, M. Klene, X. Li, J.E. Knox, H.P. Hratchian, J.B. Cross, V. Bakken, C. Adamo, J. Jaramillo, R. Gomperts, R.E. Stratmann, O. Yazyev, A.J. Austin, R. Cammi, C. Pomelli, J.W. Ochterski, P.Y. Ayala, K. Morokuma, G.A. Voth, P. Salvador, J.J. Dannenberg, V.G. Zakrzewski, S. Dapprich, A.D. Daniels, M.C. Strain, O. Farkas, D.K. Malick, A.D. Rabuck, K. Raghavachari, J.B. Foresman, J.V. Ortiz, Q. Cui, A.G. Baboul, S. Clifford, J. Cioslowski, B.B. Stefanov, G. Liu, A. Liashenko, P. Piskorz, I. Komaromi, R.L. Martin, D.J. Fox, T. Keith, M.A. Al-Laham, C.Y. Peng, A. Nanayakkara, M. Challacombe, P.M.W. Gill, B. Johnson, W. Chen, M.W. Wong, C. Gonzalez, J.A. Pople, *GAUSSIAN 03*, Revision C.02, Gaussian Inc., Wallingford, CT, 2004.
- [46] Roy Dennington II, Todd Keith, John Millam, Ken Eppinnett, W. Lee Hovell, Ray Gilliland, Semichem, Inc., GaussView, Version 3.09, Shawnee Mission, KS, 2003.
- [47] R.E. Easton, D.J. Giesen, A. Welch, C.J. Cramer, D.G. Truhlar, *Theor. Chim. Acta* 93 (1996) 281.
- [48] P.J. Hay, W.R. Wadt, *J. Chem. Phys.* 82 (1985) 270.
- [49] W.R. Wadt, P.J. Hay, *J. Chem. Phys.* 82 (1985) 284.
- [50] P.J. Hay, W.R. Wadt, *J. Chem. Phys.* 82 (1985) 299.